

# ClusterStyle: Modeling Intra-Style Diversity with Prototypical Clustering for Stylized Motion Generation

Kerui Chen<sup>1,\*</sup>, Jianrong Zhang<sup>2,\*</sup>, Ming Li<sup>3</sup>, Zhonglong Zheng<sup>4</sup>, Hehe Fan<sup>1,†</sup>

<sup>\*</sup>Equal Contribution <sup>†</sup>Corresponding author

<sup>1</sup>CCAI, Zhejiang University <sup>2</sup>ReLER, AAIL, University of Technology Sydney

<sup>3</sup>Guangming Laboratory, China <sup>4</sup>Zhejiang Normal University

<https://1233chen.github.io/ClusterStyle/>

## Abstract

Existing stylized motion generation models have shown their remarkable ability to understand specific style information from the style motion, and insert it into the content motion. However, capturing intra-style diversity, where a single style should correspond to diverse motion variations, remains a significant challenge. In this paper, we propose a clustering-based framework, **ClusterStyle**, to address this limitation. Instead of learning an unstructured embedding from each style motion, we leverage a set of prototypes to effectively model diverse style patterns across motions belonging to the same style category. We consider two types of style diversity: global-level diversity among style motions of the same category, and local-level diversity within the temporal dynamics of motion sequences. These components jointly shape two structured style embedding spaces, i.e., global and local, optimized via alignment with non-learnable prototype anchors. Furthermore, we augment the pretrained text-to-motion generation model with the Stylistic Modulation Adapter (SMA) to integrate the style features. Extensive experiments demonstrate that our approach outperforms existing state-of-the-art models in stylized motion generation and motion style transfer.

## 1. Introduction

Stylization is an essential technique for generative modeling [18, 71], enabling the rendering of source content in a target style. In the stylized motion generation [42, 58, 59], the primary aim is to transfer the style from a reference motion sequence to a source motion sequence while preserving the original content, which makes it useful in various real-world applications, including augmented reality [59], animation [1], and virtual avatars [3].

Motion style is inherently expressive [4, 82], where the same style can exhibit diverse motion variations influenced

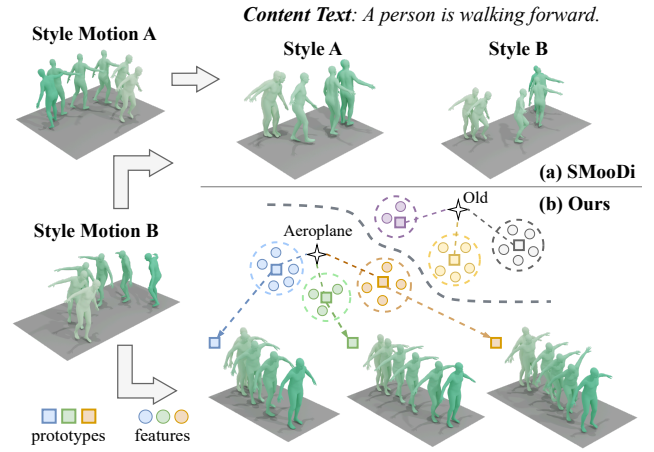


Figure 1. Comparison between SMooDi [81] and ClusterStyle. Given two style motions with the same style but differing in expression, along with a content text, (a) SMooDi generates similar stylized motions. Meanwhile, the generated motions still reflect elements from the style motions’ content, leading to inconsistency with the intended content text. (b) In contrast, using **different prototypes** corresponding to the aeroplane style, our method generates diverse motion results with varying extent and better preserves the semantics of the content text.

by the human’s mood, intention, or context. For example, given a textual description “a person is walking forward”, the “aeroplane” style should encompass a wide range of postures as well as variations in action amplitude, rather than a single rigid walk with both arms raised.

Recently, many works aim to achieve stylized motion generation and motion style transfer using diffusion models [25, 27, 36, 51, 53, 56, 57, 81]. Song et al. [57] leveraged trajectory as an auxiliary condition during the denoising process to improve the preservation of the content. SMooDi [81] introduces a large-scale dataset for stylized motion generation from both the textual description and style motion. Building on the pretrained text-to-motion model, i.e., MLD [9], it uses a ControlNet-like architecture

to serve as the style encoder. BiFlow [36] further replaces the style-to-content flow with a bidirectional control flow to reduce conflicts between content and style.

However, these methods embed the style motion into an *unstructured* feature, which often cannot model the intra-style diversity, resulting in relatively uniform motion output. Meanwhile, we find that such unstructured features include both content and style information of the style motion, and the content part may lead to deviations from the target content intended by the text. For example, in Figure 1(a), given two style motions with the same style but to different extents, and a text prompt “a person is walking forward”, SMooDi generates relatively uniform motions, and does not reflect “walking forward”.

In this paper, we propose ClusterStyle to address these limitations. It is inspired by recent clustering-based representation learning methods [38, 83] in computer vision, where cluster centers are progressively updated through interactions with pixel features. Specifically, each style category is represented by clustering its style motions into  $K$  non-learnable prototypes (*i.e.*, distinct centroids). Then, we build a transformer-based architecture as the style motion encoder, and the extracted features are used to update the prototypes iteratively during training. To facilitate the learning of a high-quality and disentangled style feature space, we encourage the contrastive property across prototypes belonging to different categories (Prototype-Based Inter-Style Learning) as well as among distinct prototypes within the same category (Prototype-Based Intra-Style Learning). Furthermore, we observe that a single motion sequence may also exhibit stylistic differences over time. Thus, we propose hierarchical clustering, which performs clustering on the entire motion sequences (*global-level*) as well as their temporal segments (*local-level*). Finally, we present a Stylistic Modulation Adapter (SMA) to effectively integrate the style information into the text-to-motion model.

Our approach characterizes two appealing advantages. First, we explicitly model the intra-style diversity through learning multiple clustering centroids on both global and local levels of motion sequences. As shown in Figure 1(b), using **different cluster centroids** (prototypes), our method can generate expressions of the same style to varying extents, making ClusterStyle a flexible and *interpretable* framework. Second, such prototypes focus more on style attributes, enabling a better consistency between the motion and the target content described by the text. We evaluate the proposed approach on the 100STYLE [81] and HumanML3D [21] datasets across two tasks, *i.e.* stylized motion generation and motion style transfer. Extensive experiments demonstrate that ClusterStyle outperforms current state-of-the-art methods in fidelity and content preservation.

Our contributions can be summarized as follows: **1.** We propose ClusterStyle, a clustering-based framework that fa-

cilitates diverse stylized motion generation. **2.** We propose to use multiple clustering-based prototypes to model the intra-style diversity and consider both global-level and local-level discrepancies. **3.** We introduce Stylistic Modulation Adapter (SMA) for style attribute injection.

## 2. Related Work

**Text-to-Motion Generation.** The task of generating human motion from textual descriptions has seen rapid advancement in recent years. Early studies primarily focus on constructing a shared embedding space for text and motion [2, 19, 46–48, 60]. Further advancements introduce the idea of discretizing the motion representation through vector quantization [22]. For instance, T2M-GPT [74] presents VQ-VAE and GPT along with some training recipes, *e.g.*, corruption strategy, which significantly improve the performance on the large-scale dataset, *i.e.*, HumanML3D [21]. Based on this line, several works improve this paradigm by enhancing the VQ-VAE [23, 80] and leveraging masked token modeling [23, 49, 50].

Recently, diffusion models have become an increasingly popular choice for motion generation. The foundation of the diffusion model in this domain is laid by MDM [61] and MotionDiffuse [78]. They both use the Transformer-based denoising network to progressively refine random noises to synthesize human motions guided by textual descriptions. Subsequent works [11, 20, 31, 64, 65, 68] introduce diverse additional information to improve the quality or controllability of motion generation, such as spatial constraints [33, 62, 67], physical constraints [72] and multimodal information [26, 77, 84]. MLD [9] proposes to shift the diffusion process to the latent space. The following efforts have been dedicated to improving performance [17, 75] and sampling efficiency [79] through architectural refinement. Motion latent diffusion model is more relevant to our approach, as the current stylized motion generation methods are built upon MLD [9]. We augment this architecture with our designed Stylistic Modulation Adapter (SMA) to effectively fuse text and style.

**Stylized Motion Generation.** Stylized motion generation aims to synthesize human motions that reflect a desired content and style, which can be specified through text [35, 56] or reference motion [42, 45, 51, 58, 59, 66, 69]. Earlier approaches [1, 29] primarily focused on motion style transfer and employed autoencoder-based architectures with AdaIN [28] to disentangle and recombine content and style features. Following this, Guo [24] explored style transfer in a probabilistic latent space, while MOST [34] improves the recombination technique between the content and style. Recently, diffusion-based methods [27, 53, 57] have increasingly been adopted in this task, primarily leveraging the prior knowledge from pre-trained text-to-motion models.

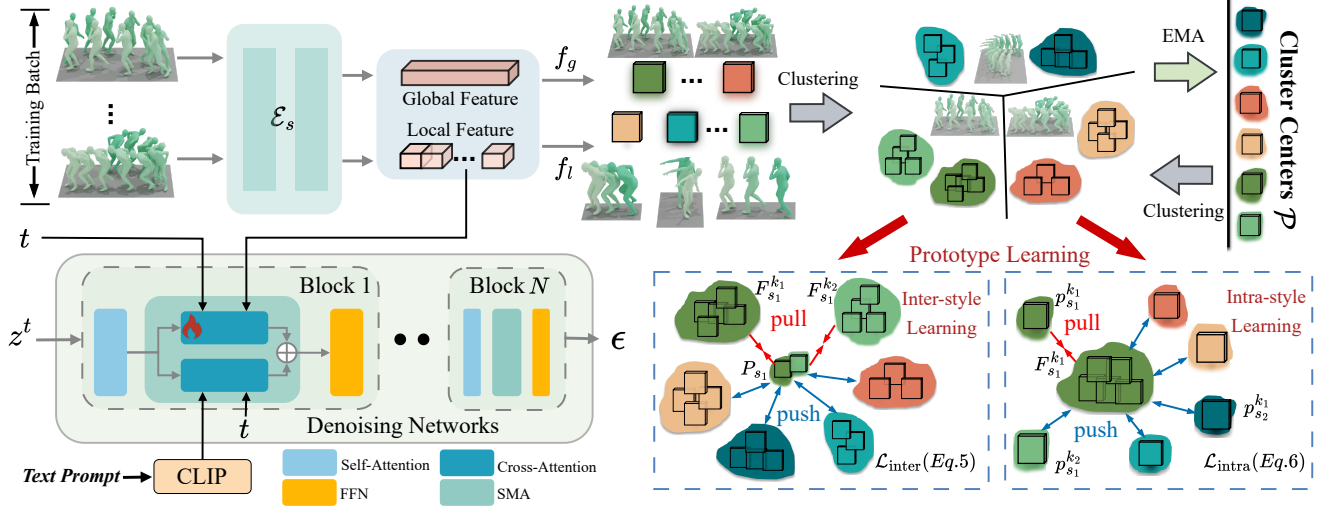


Figure 2. The overview of the ClusterStyle. Our method consists of a style encoder and a motion latent diffusion model. In the style encoder, we present a cluster-based prototype learning paradigm that represents each style category using a set of non-learnable prototypes (cluster centers) to model the intra-style diversity explicitly. Then, two contrastive losses are proposed for prototype-based intra-style learning and inter-style learning, respectively. To incorporate the style embedding into the diffusion process, we introduce a Style Modulation Adapter (SMA), enabling effective guidance of stylized motion generation.

For instance, Hu et al. [27] treat the denoising process as a style transfer stage and utilize CLIP [54] for transfer guidance, and MoMo [53] achieves zero-shot style transfer by exploring the attention mechanism.

To facilitate research in this area, SMooDi [81] proposes a new dataset named 100STYLE, which is paired with content text and style motion for a style-specific task. In addition to introducing a new dataset, SMooDi proposed a ControlNet-like architecture to incorporate style features into the generation process. To mitigate conflicts between content and style, BiFlow [36] refines the style-to-content flow in the SMooDi into a bidirectional control flow. Style-Motif [25] leverages multi-modal style inputs (e.g., text, audio, motion) and proposes a style-content cross-fusion mechanism to effectively integrate this information.

However, these methods all neglect the importance of intra-style diversity, leading to the lack of diversity and distinctiveness in the generated results when guided by different style motions. In this paper, we represent each style category with multiple prototypes, obtained by clustering style embeddings from the full style motion dataset, which are used to model the intra-diversity of style.

**Clustering in Vision.** Clustering enables models to automatically mine underlying patterns and learn meaningful representations from data. Early clustering methods [16, 32, 55] primarily relied on raw data representations and hand-crafted priors, which were not effective when faced with complex data. Some methods [5, 6, 12, 70] propose to combine deep learning techniques with prototype-based clustering. For example, Wang et al. [63] considered the represen-

tation learning from the clustering perspective, constructing multiple cluster centers for each class to improve the recognition ability of the model. This clustering paradigm has inspired a broad spectrum of research across domains, such as image segmentation [7, 13, 37, 38, 44, 73, 83], point cloud analysis [14, 15, 39, 40], and zero-shot learning [41, 52].

Inspired by these methods, we extend the clustering technique to stylized motion generation. Different from previous works that focus on global information of each data instance (i.e., image), ClusterStyle considers both long-term and short-term relationships within style motion sequences, facilitating a more fine-grained understanding of underlying style attributes and expression patterns.

### 3. Method

In this paper, we aim to model intra-style diversity for stylized 3D motion generation. As illustrated in Figure 2, we introduce ClusterStyle, a novel framework that comprises a motion latent diffusion model and a style encoder with a cluster-based prototype learning strategy. Section 3.1 outlines the problem formulation and provides an overview of our approach. We introduce cluster-based style prototype learning, hierarchical style modeling, and style modulation adapter in Section 3.2, 3.3, and 3.4, respectively. Finally, implementation details are provided in Section 3.5.

#### 3.1. Problem Setting and Overview

Given a style motion sequence  $\mathbf{X}_s = [\mathbf{x}_s^1; \mathbf{x}_s^2; \dots; \mathbf{x}_s^{L_s}]$  and a content text  $c$ , where  $\mathbf{x}_s^i \in \mathbb{R}^d$ ,  $L_s$  and  $d$  are the length and dimension of style motion. Our goal is to generate a

motion sequence  $\mathbf{X}_c = [\mathbf{x}_c^1; \mathbf{x}_c^2; \dots; \mathbf{x}_c^{L_c}]$  with length  $L_c$  that is consistent with the text while adhering to the style demonstrated by the style motion  $\mathbf{X}_s$ .

Specifically, following previous works [25, 36, 81], we build our approach on a motion latent diffusion model [9], which consists of a VAE and latent diffusion model, pre-trained on the HumanML3D dataset [21]. During training, with the style motion-text pair  $\{\mathbf{X}_s, c_s\}$  available, we first feed the style motion into the VAE encoder to obtain the latent feature  $z_s$ . We gradually add Gaussian noise  $\epsilon$  to  $z_s$  over  $T$  times via  $z_s^t = \sqrt{\alpha^t} z_s^0 + \sqrt{1 - \alpha^t} \epsilon$ , where  $t$  is the timestep and  $\{\alpha^t\}_{t=0}^T$  is the noise variance schedule. Then, we propose a clustering-based style encoder which uses a set of prototypes to represent a single style class for intra-style diversity (Section 3.2). It also captures style information hierarchically by modeling both global-level motion and local-level temporal segments (Section 3.3), obtaining the style embedding  $f_s$ . Then, we train a denoising autoencoder to predict the noise conditioned on  $f_s$  and  $c_s$ , the loss function can be formulated as:

$$\mathcal{L}_{\text{diff}}^s = \mathbb{E}_{z_s, \epsilon, t, c_s, f_s} [\|\epsilon - \epsilon_\theta(z_s^t, t, c_s, f_s)\|_2^2]. \quad (1)$$

Furthermore, to prevent forgetting content-related prior knowledge, we also train the diffusion model on the content motion-text pair  $\{\mathbf{X}_c, c\}$  from the HumanML3D dataset,

$$\mathcal{L}_{\text{diff}}^c = \mathbb{E}_{z_c, \epsilon, t, c, f_c} [\|\epsilon - \epsilon_\theta(z_c^t, t, c, f_c)\|_2^2], \quad (2)$$

where  $z_c$  and  $f_c$  denote the motion latent features from the VAE encoder and the style encoder, respectively. Different from existing methods [81] that employ a ControlNet-like [76] architecture for style feature fusion, we utilize a cross-attention to understand the textual description [75] and further propose a Style Modulation Adapter (Section 3.4) for style feature integration.

Combining these components, we optimize ClusterStyle using the following overall training objective:

$$\mathcal{L}_{\text{total}} = \mathcal{L}_{\text{diff}}^s + \mathcal{L}_{\text{diff}}^c + \lambda_{\text{style}} \mathcal{L}_{\text{style}}, \quad (3)$$

where  $\lambda$  is a hyper-parameter to balance the weight of  $\mathcal{L}_{\text{style}}$ , which supervises the training of the style encoder (see Section 3.3 for more details).

### 3.2. Clustering-based Style Prototype Learning

The design of ClusterStyle is motivated by a key insight: motion style is inherently diverse, a single style should not be confined to a fixed form, but can manifest through multiple dynamic patterns. To achieve this, we raise two questions: ❶ *How to model the intra-style diversity?* ❷ *How can intra-style diversity be automatically mined without relying on manual annotation?* To answer these questions,

we propose a clustering-based framework for style prototype learning, which enables the discovery of underlying sub-style patterns within each style category.

**Cluster Center Initialization.** As a response to question ❶, we propose to represent each style category using multiple prototypes. Each prototype captures a distinct sub-style pattern and acts as a reference point that encourages variation within the same style. This helps organize the style features into a well-structured and diverse style space. Specifically, for a style category  $s$ , we assume it contains  $K_g$  sub-style patterns and define a cluster using a set of prototypes (*a.k.a.* cluster centers)  $P_s = \{p_s^i\}_{i=1}^{K_g}$ , where  $p_s^i \in \mathbb{R}^{1 \times d'}$  and  $d'$  is the dimension of the prototype. We encode the style motion feature using a transformer-based style encoder  $\mathcal{E}_s$ , which can be computed as  $f_g = \mathcal{E}_s(\mathbf{X}_s)$ . Our goal is to map the style feature  $f_g$  to the closest prototype within  $P_s$ , which represents the corresponding style cluster. To extend this idea, the prototype clusters for all style categories are collectively defined as  $\mathcal{P} = \{P_s\}_{s=1}^S$ , where  $S$  is the total number of style categories.

**Prototype Assignment.** It is challenging to directly supervise the assignment of features to prototypes due to the lack of manual annotations that specify or differentiate these prototypes. Driven by question ❷, we formulate this process as an unsupervised optimal transport problem. Formally, given a series of style motion features  $F_s = [f_{g,s}^1, f_{g,s}^2, \dots, f_{g,s}^{N_s}] \in \mathbb{R}^{d' \times N_s}$ , where  $N_s$  denotes the total motion numbers of the style category  $s$ . Correspondingly, we define a prototype matrix  $P'_s \in \mathbb{R}^{d' \times K_g}$  representing  $K_g$  style-specific prototypes. Note that each column of  $F_s$  and  $P'_s$  is L2-normalized. Based on a binary assignment matrix  $L_s \in \{0, 1\}^{K_g \times N_s}$ , we compute the prototype assignment map as  $A_s = P'_s L_s \in \mathbb{R}^{d' \times N_s}$ , where each column of  $A_s$  represents the aggregated prototype assigned to the corresponding style motion feature. We measure the inner product similarity  $\langle \cdot, \cdot \rangle_I$  and maximize  $\langle A_s, F_s \rangle_I$  to determine  $L_s$ . To prevent all style motion features from being assigned to a single prototype, we introduce a balancing constraint that encourages each prototype to be selected approximately  $\frac{N_s}{K_g}$  times on average. We adopt the Sinkhorn algorithm [10] to solve this problem, which introduces entropy regularization to enable fast and stable computation of the transport plan:

$$\max_{L_s} \langle A_s, F_s \rangle_I + \mu \text{KL}(L_s \| \frac{1}{K_g N_s} \mathbf{1}_{K_g} \mathbf{1}_{N_s}^\top), \quad (4)$$

where KL is used to smooth the distribution via a hyper-parameter  $\mu$ . There are two additional constraints imposed on relaxed  $L_s$ : (1)  $L_s \in \mathbb{R}_+^{K_g \times N_s}$  ensuring that each feature is assigned once; and (2)  $L_s \mathbf{1}_{N_s} = \frac{N_s}{K_g} \mathbf{1}_{K_g}$ , encouraging balanced usage of prototypes.

**Prototype-based Contrastive Learning.** After tackling questions ❶ and ❷, the next step aims to learn the high-



quality representation of  $\mathcal{P}$  and style motions. We propose two prototype-based contrastive losses  $\mathcal{L}_{\text{inter}}^g$  and  $\mathcal{L}_{\text{intra}}^g$ , corresponding to Prototype-based Inter-Style Learning and Prototype-based Intra-style Learning, respectively. Specifically, with the style motion feature  $f_g$ , the prototype-based inter-style learning is designed to enhance inter-style discrimination by pulling each motion feature closer to the prototype of its style category and pushing it away from prototypes of all other styles. The inter-style contrastive loss  $\mathcal{L}_{\text{inter}}^g$  is formulated as follows:

$$\mathcal{L}_{\text{inter}}^g = -\log \frac{\exp(-\text{sim}[f_g, s])}{\sum_{s'=1}^S \exp(-\text{sim}[f_g, s'])}, \quad (5)$$

where  $\text{sim}[f_g, s] = \min\{\cos(f_g, p_s^k)\}_{k=1}^{K_g}$  is a function to measure the similarity between the style feature  $f_g$  and  $P_s$ ,  $\cos(\cdot)$  denotes the cosine similarity. We provide an ablation study in the Appendix to evaluate the impact of different similarity metrics on model performance.

In prototype-based intra-style learning, each motion feature is contrasted against all prototypes by treating the assigned prototype as positive, and all others, even within the same style category, as negatives. Given the style motion feature  $f_g$ , the corresponding prototype  $p_s^k$ , we define the negative prototypes as  $\hat{P}$ , which consists of all prototypes in  $\mathcal{P}$  except the assigned  $p_s^k$ . Then, the intra-style contrastive loss  $\mathcal{L}_{\text{intra}}^g$  can be written as:

$$\mathcal{L}_{\text{intra}}^g = -\log \frac{\exp(\cos(f_g, p_s^k)/\tau)}{\exp(\cos(f_g, p_s^k)/\tau) + \sum_{\hat{p} \in \hat{P}} \beta \exp(\cos(f_g, \hat{p})/\tau)}, \quad (6)$$

where  $\beta = 1$  if  $\hat{p} \not\sim f_g$ , else 5,  $\not\sim$  indicates that  $\hat{p}$  and  $f_g$  are from different style categories,  $\tau$  is a temperature hyper-parameter which is set to 0.05 following [8]. Then, the final training objective is defined as follows:

$$\mathcal{L}_{\text{style}}^g = \mathcal{L}_{\text{inter}}^g + \mathcal{L}_{\text{intra}}^g. \quad (7)$$

By doing so, the proposed two loss functions encourage the model to focus more on style-relevant patterns and to learn style representations that are disentangled from content information, thereby preventing the target content from being influenced by content information embedded in the style motion.

**Prototype Update.** Unlike traditional classifiers optimized by gradient descent, our prototypes are non-parametric and non-learnable statistics computed as the centroids of their assigned style-feature sets. Concretely, for category  $s$  and prototype  $k$ , let  $\hat{f}_{g,s}^k$  denote the mean of features assigned to that prototype. At each training iteration, we update the prototype  $p_s^k$  by EMA via below formula:

$$p_s^k \leftarrow \lambda_p p_s^k + (1 - \lambda_p) \hat{f}_{g,s}^k, \quad (8)$$

where  $\lambda_p \in [0, 1]$  is a momentum coefficient.

**Prototype-based Guidance.** The prototypes can serve as guiding signals to generate diverse stylized motion. Specifically, we define the prototype-based guidance function

$$\epsilon_\theta(z^t, t, c, s) = \epsilon_\theta(z^t, t, c, s) + \gamma_g \nabla_{z^t} G_g(z^t, t, p_s^k), \quad (9)$$

where  $G_p(z^t, t, p_s^k) = 1 - \cos(f_g^{x^0}, p_s^k)$ ,  $\gamma_g$  is the guidance weight. During the inference,  $z^t$  is iteratively optimized to approach the sub-style pattern associated with the target prototype  $p_s^k$ . Here,  $z^t$  is the noisy latent at the timestep  $t$ , and we transform it to  $z^0$  using the predict noise, which is then decoded into  $x^0$  through  $\mathcal{D}(z^0)$ .  $f_g^{x^0}$  is the style feature of  $x^0$ , and  $\cos(\cdot)$  denotes the cosine similarity. Please find more details in the Appendix.

### 3.3. Hierarchical Style Modeling

It is worth noting that motion inherently exhibits temporal dynamics where a single motion sequence may involve stylistic variations over time. To capture a fine-grained understanding of style patterns within a motion sequence, we propose a hierarchical style modeling framework that independently clusters features at both the global level (entire motion sequences) and the local level (temporal segments). Specifically, as we mentioned in Section 3.2, we encode the style motion sequence  $X_s$  into  $f_m \in \mathbb{R}^{L_s \times d'}$ , the global style embedding  $f_g$  is processed by an average pooling operation over the temporal dimension. For the local style embedding, we first divide  $f_m$  into  $L_w$  non-overlapping temporal segments with a window size of  $w$ , where  $L_s = L_w \times w$ . Then we apply the same pooling operation within each segment, obtaining  $f_l \in \mathbb{R}^{L_w \times d'}$ . We perform an identical clustering-based learning that clusters the local-level features into  $K_l$  local prototypes. A prototype-based contrastive loss,  $\mathcal{L}_{\text{style}}^l$ , is then computed to guide the learning of fine-grained style representations. The final style loss  $\mathcal{L}_{\text{style}}$  is formulated as follows:

$$\mathcal{L}_{\text{style}} = \mathcal{L}_{\text{style}}^g + \mathcal{L}_{\text{style}}^l. \quad (10)$$

Finally, the overall style representation  $f_s \in \mathbb{R}^{(L_w+1) \times d'}$ , which encapsulates both hierarchical information and intra-style diversity, is constructed by concatenating the global-level feature  $f_g$  and local-level features  $f_l$ , and is subsequently used to control the style in the generation process. Note that the guidance mechanism (Section 3.2, Eq. 9) used in the global prototype approach can also be applied to local prototypes.

### 3.4. Style Modulation Adapter

With the style representation  $f_s$  available, we design a Style Modulation Adapter (SMA) to effectively integrate  $f_s$  into the pre-trained text-to-motion model, while preserving its prior knowledge. As shown in Figure 2, the proposed SMA takes both text embedding  $c$  and style representation  $f_s$  as

Methods	Venue	FID ↓	FSR ↓	MM Dist ↓	R-Precision (Top-3) ↑	Diversity →	SRA ↑
Motion Puzzle [29]	TOG 2022	6.127	0.185	6.467	0.290	6.576	63.769
Aberman [1]	TOG 2020	3.309	0.347	5.983	0.406	8.816	54.367
ChatGPT+MLD	-	0.614	0.131	4.313	0.605	8.836	4.819
SMooDi [81]	ECCV 2024	1.609	0.124	4.477	0.571	9.235	72.418
BiFlow [36]	ARXIV 2025	<u>1.527</u>	0.118	<u>4.292</u>	<u>0.613</u>	9.303	77.042
StyleMotif [25]	ARXIV 2025	1.551	<b>0.097</b>	4.354	0.586	7.567	<u>77.650</u>
ClusterStyle (Ours)	-	<b>1.137</b>	<u>0.113</u>	<b>3.610</b>	<b>0.708</b>	8.719	<b>78.101</b>

Table 1. Quantitative comparisons of ClusterStyle with existing state-of-the-art methods on the stylized motion generation task. The best and second best results are **bold** and underlined.

conditions. It employs two cross-attention modules for the content branch and style branch, respectively, enabling separate control over semantic content and stylistic rendering. Specifically, in the content branch, the text embedding is first computed with  $O_{\text{content}} = \text{Softmax}(\frac{QK^\top}{\sqrt{d}})V$  to obtain the content feature, where  $Q = XW_c^q$ ,  $K = cW_c^k$ ,  $V = cW_c^v$  with  $W_c^{q,k,v} \in \mathbb{R}^{d \times d}$ . As for the style branch, we use another cross-attention to model the interaction between  $f_s$  and the denoised latent motion  $z$ , which can be calculated as  $O_{\text{style}} = \text{Softmax}(\frac{Q(K')^\top}{\sqrt{d}})V'$ , where  $K' = f_s W_s^k$ ,  $V' = f_s W_s^v$  with  $W_s^{k,v} \in \mathbb{R}^{d' \times d}$ . We then combine  $O_{\text{content}}$  and  $O_{\text{style}}$  together, leading to the output  $O_{\text{SMA}}$

$$O_{\text{SMA}} = O_{\text{content}} + \lambda O_{\text{style}}, \quad (11)$$

where  $\lambda$  is a trainable parameter that modulates the balance between content and style.

### 3.5. Implementation Details

ClusterStyle adopts a frozen CLIP ViT-L/14 model as the text encoder. For the style encoder, we use 6 transformer layers with a dimension of 512. We set the global prototype number  $K_g$  to 3, the local prototype number  $K_l$  to 30, and the momentum coefficient  $\lambda_p$  to 0.95. Following [75], we use a pretrained VAE with 5 latent vectors. The denoising autoencoder consists of  $N = 9$  layers of transformer blocks with a dimension of  $d = 256$ . During training, ClusterStyle is optimized using the AdamW optimizer with a batch size of 128, and the learning rate is set to 2e-5 with a linear warm-up period of 500 iterations, followed by 3000 iterations of training with a constant learning rate. We first train the style encoder for 1800 iterations, after which prototype updates are frozen during the remaining training process. Training our model takes about 1 hour on a single NVIDIA A6000 GPU. Note that only  $W_s^{k,v}$  in the Style Modulation Adapter (SMA) and parameters in the style encoder are updated. During inference, we generate stylized motions over 50 steps using the DDIM strategy. Following SMooDi [81], we use classifier-free guidance for content texts and classi-

fier guidance for style motions. Please find more information corresponding to the inference in the Appendix.

## 4. Experiment

### 4.1. Experimental Settings

We evaluate our approach on two tasks: stylized motion generation (Section 4.2) and motion style transfer (Section 4.3). We compare our model with five representative state-of-the-art methods: Aberman [1], Motion Puzzle [29], SMooDi [81], BiFlow [36], and StyleMotif [25]. Meanwhile, we also offer detailed analysis and discussion in Section 4.4. Please note that more information about datasets is provided in the Appendix.

**Datasets.** We conduct experiments using a single model on two datasets, *i.e.*, HumanML3D [21] and 100STYLE [81]. HumanML3D [21] is used to preserve content-related prior knowledge. 100STYLE [81] is used for providing a wide range of motion styles to guide style-specific learning. During evaluation, content is derived from HumanML3D, while style references are taken from 100STYLE. Please see the Appendix for more information.

**Evaluation Metrics.** Following SMooDi [81], we adopt standard evaluation metrics to comprehensively assess the quality of stylized motion. These metrics include: (1) R-Precision and Multi-modal Distance (MM-Dist) for content preservation; (2) Style Recognition Accuracy (SRA) for style fidelity; (3) Fréchet Inception Distance (FID) for motion quality; (4) *Diversity* for motion diversity; (5) Foot Skating Ratio (FSR) for physical plausibility.

### 4.2. Stylized Motion Generation

**Quantitative Results.** Table 1 shows quantitative results on the HumanML3D and 100STYLE datasets. We compare our method with current state-of-the-art methods, *e.g.*, SMooDi [81], BiFlow [36], and StyleMotif [25]. Our method achieves R-Precision of 0.708 and SRA of 78.101, surpassing the BiFlow by 15.5% and 1.1%. In terms of FID, our method achieves a score of 1.137, representing a 27% improvement over StyleMotif and demonstrating sig-

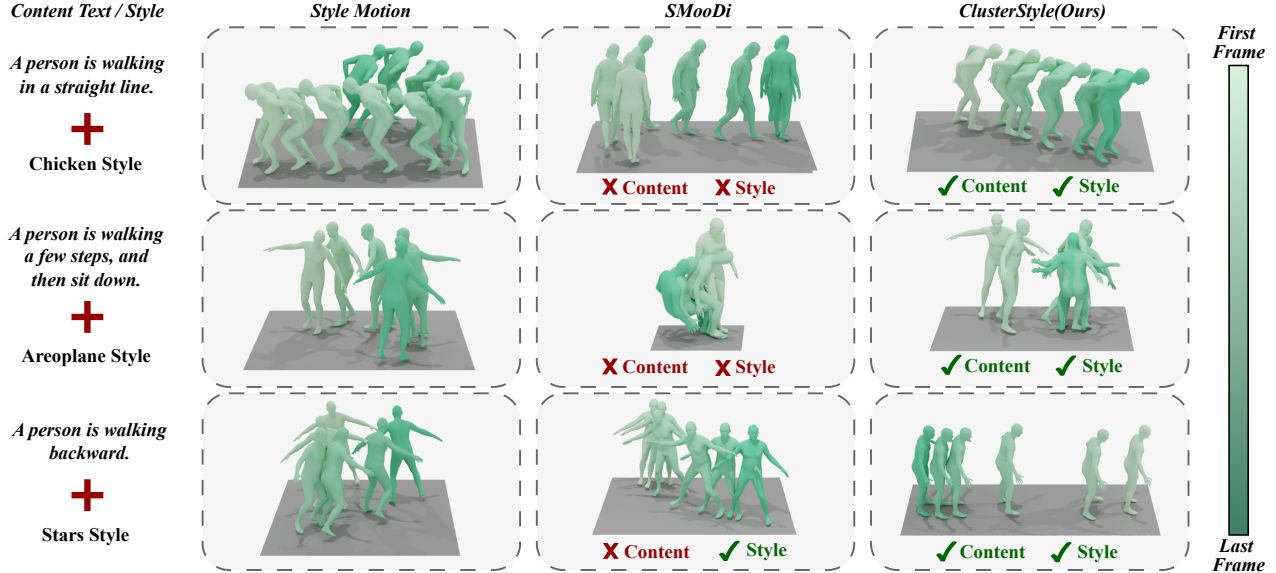


Figure 3. Qualitative results of stylized motion generation. We compare our method with SMooDi under various text prompts and style motion inputs. Our approach demonstrates better content alignment and achieves more accurate and expressive style rendering. For example, the results of SMooDi are inconsistent with the motion trajectories (e.g., "backward", "straight") and action (e.g., "walk") described in the content. More visual comparisons can be found in the website.

Method	FSR ↓	FID ↓	SRA ↑
Motion Puzzle [29]	0.197	6.871	67.233
Aberman [1]	0.338	3.892	61.006
SMooDi [81]	0.095	1.582	65.147
BiFlow [36]	<u>0.087</u>	1.566	<u>70.238</u>
StyleMotif [25]	0.094	<u>1.375</u>	68.810
ClusterStyle (Ours)	<b>0.078</b>	<b>0.768</b>	<b>73.849</b>

Table 2. Quantitative comparison with the state-of-the-art methods on the style transfer task.

nificantly improved generation fidelity. These results show that the motions generated by our approach are semantically aligned with the content text and stylistically consistent with the reference style motion.

**Qualitative Results.** In Figure 1, we present visual comparisons between our model and baseline approach SMooDi [81]. It can be seen that SMooDi struggles to retain essential motion details (e.g., "circular" or "walking" trajectories) and lacks fidelity in expressing target styles such as "aeroplane" or "chicken". Our approach is able to generate motions that better reflect the semantics of the text prompt, while also transferring correct stylistic characteristics from the reference motion. These observations demonstrate the superior performance of our model, as well as its effectiveness in disentangling motion content and style.

### 4.3. Motion Style Transfer

Our method utilizes SD-Edit [43] to achieve motion style transfer, relying solely on the pre-trained ClusterStyle

model without additional fine-tuning. More implementation details are available in the Appendix.

**Quantitative Results.** Table 2 presents the quantitative results, comparing our method against current state-of-the-art methods. Our method achieves the lowest Foot Skating Ratio (0.078), reflecting a 17% reduction compared to the best-performing method, i.e., StyleMotif, and indicating improved physical realism. For FID and SRA, our methods achieve scores of 0.768 and 73.849, a 44% and 5.03% improvement over StyleMotif, demonstrating superior motion fidelity and transfer accuracy.

**Qualitative Results.** Figure 4 shows the visual results of ClusterStyle on motion style transfer. Given styles of "chicken" and "star", we observe that our method effectively preserves the action and trajectory of the content motion, while integrating styles consistent with style motions.

### 4.4. Discussion

**Style Diversity.** We explore the capability of our method to generate diverse motions from a single style. In our experiments, we use different global prototypes as global style features to generate stylized motions, as shown in the left column of Figure 5. Furthermore, we randomly permute and combine local prototypes to generate stylized motions, as shown in the right column of Figure 5. We find that both different global prototypes and permutations of local prototypes yield stylistic results that vary in the extent of spread arms. Please note that, at inference time, our method enables diverse motion generation by integrating the style features obtained from the style encoder with different config-

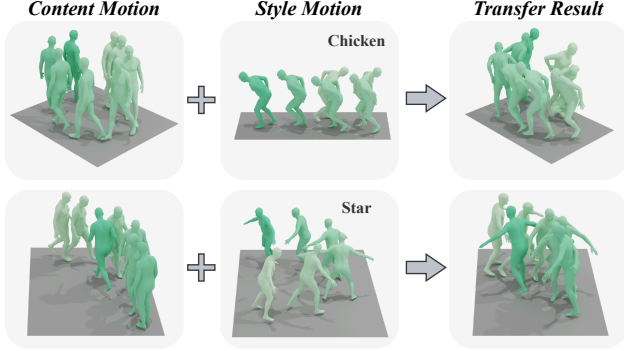


Figure 4. Qualitative results of motion style transfer. Our approach effectively transfers the target motion style, such as ‘Chicken’ or ‘Star’, onto the original motion, preserving its structure while adapting its stylistic characteristics.

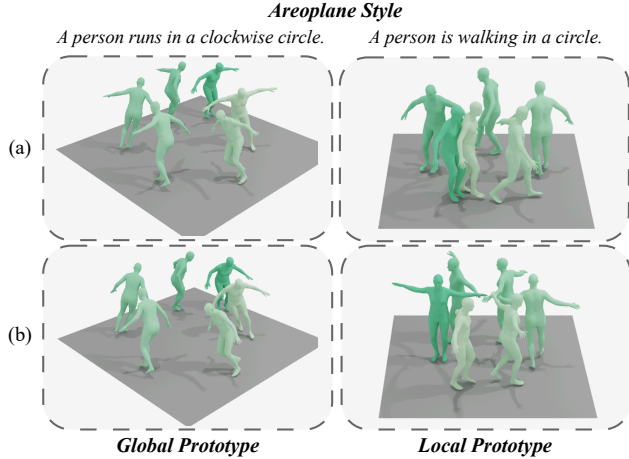


Figure 5. Visualization of prototype guiding. We visualize how global and local prototypes guide the stylization process for diverse generation results under the ‘Aeroplane’ style. (a) Global prototype; (b) Local prototype.

$K_g$	$K_l$	FID ↓	MM Dist ↓	R-Precision ↑ (Top-3)	Diversity →	SRA ↑
1	1	1.443	3.886	0.668	8.136	74.785
1	30	1.143	3.613	0.701	8.483	76.226
3	30	<b>1.137</b>	<b>3.610</b>	<b>0.708</b>	8.719	78.101
5	30	1.170	3.641	0.701	8.366	77.883
10	30	1.198	3.687	0.697	8.183	<b>78.528</b>
3	1	1.313	3.769	0.685	8.178	<b>78.744</b>
3	5	1.226	3.690	0.695	8.461	78.399
3	10	1.185	3.637	0.701	8.661	77.281
3	30	<u>1.137</u>	<u>3.610</u>	<u>0.708</u>	8.719	<u>78.101</u>
3	50	<b>1.092</b>	<b>3.607</b>	<b>0.711</b>	8.516	77.302

Table 3. Ablation studies of key components.

urations of global and local prototypes. More visual results are provided in the website.

**Investigating Key Components.** We first investigate the

$\mathcal{L}_{\text{style}}$	FID ↓	R-Precision ↑ (Top-3)	Diversity →	SRA ↑
$\mathcal{L}_{\text{inter}}$	1.112	0.712	8.479	75.182
$\mathcal{L}_{\text{intra}}$	1.349	0.673	8.509	67.746
$\mathcal{L}_{\text{entropy}}$	1.331	0.677	8.886	65.465
$\mathcal{L}_{\text{inter}} + \mathcal{L}_{\text{intra}}$	1.137	0.708	8.719	78.101

Table 4. Ablation studies of different loss functions for the style encoder.

effectiveness of the clustering strategy and prototype number (i.e.,  $K_g$  and  $K_l$ ) on the task of stylized motion generation, and the results are shown in Table 3.

**Clustering Strategy:** We replace the clustering procedure with a learnable classification head, and the style loss  $\mathcal{L}_{\text{style}}$  is replaced by a conventional cross-entropy loss. As indicated in the first row of Table 3, this modification leads to a 0.3 reduction in FID, a 5.6% decrease in R-Precision, and a 3.32% drop in SRA. This shows the effectiveness of the proposed cluster-based framework.

**Global Prototype Number  $K_g$ :** The middle four rows of Table 3 illustrate the impact of varying the number of global prototypes.  $K_g = 3$  yields relatively better results compared to other configurations. We observe a trade-off: as the number of global prototypes increases, content consistency metrics (e.g., R-Precision) tend to decline, whereas SRA improves. This suggests that while diversity benefits from a larger set of prototypes, content alignment may be negatively affected.

**Local Prototype Number  $K_l$ :** The last five rows of Table 3 show the impact of different number of local prototypes.  $K_l = 30$  achieves comparable performance to  $K_l = 50$ , while being more computationally efficient. It can be seen that increasing local prototypes improves content preservation but degrades SRA, showing an opposite trend to global prototypes.

**Ablation Study of Training Objective.** Table 4 presents the impact of different loss functions used in the style encoder. Training with only inter-style  $\mathcal{L}_{\text{inter}}$ ,  $\mathcal{L}_{\text{intra}}$  or  $\mathcal{L}_{\text{entropy}}$  leads to performance drops of 2.9%, 10.4%, and 12.6% in SRA, respectively. Here,  $\mathcal{L}_{\text{entropy}}$  denotes a variant where learnable prototypes are trained using a standard cross-entropy loss instead of  $\mathcal{L}_{\text{intra}}$ . Our prototype-based contrastive learning achieves the best performance by combining  $\mathcal{L}_{\text{inter}}$  and  $\mathcal{L}_{\text{intra}}$  together.

## 5. Conclusion

In this paper, we propose ClusterStyle, a clustering-based framework for capturing intra-style diversity in stylized motion generation. Unlike prior methods that learn a single embedding per style, ClusterStyle represents style features using multiple clustering-based prototypes at both global and local levels. To fuse style features into the pretrained diffusion model, we introduce the Stylistic Modulation Adapter (SMA). Our approach achieves superior per-



formance across stylized motion generation and motion style transfer. We conduct extensive ablation studies and provide visual results to validate the effectiveness of the proposed components. We also show that prototypes can learn diverse sub-style patterns with clear semantic meaning, enhancing both diversity and interpretability.

## References

- [1] Kfir Aberman, Yijia Weng, Dani Lischinski, Daniel Cohen-Or, and Baoquan Chen. Unpaired motion style transfer from video to animation. *ACM Transactions on Graphics (TOG)*, 39(4):64–1, 2020. 1, 2, 6, 7
- [2] Chaitanya Ahuja and Louis-Philippe Morency. Language2pose: Natural language grounded pose forecasting. In *2019 International conference on 3D vision (3DV)*, pages 719–728. IEEE, 2019. 2
- [3] Karan Ahuja, Eyal Ofek, Mar Gonzalez-Franco, Christian Holz, and Andrew D Wilson. Coolmoves: User motion accentuation in virtual reality. *Proceedings of the ACM on Interactive, Mobile, Wearable and Ubiquitous Technologies*, 5(2):1–23, 2021. 1
- [4] Syed Muhammad Abrar Akber, Sadia Nishat Kazmi, Syed Muhammad Mohsin, and Agnieszka Szczesna. Deep learning-based motion style transfer tools, techniques and future challenges. *Sensors*, 23(5):2597, 2023. 1
- [5] Mathilde Caron, Piotr Bojanowski, Armand Joulin, and Matthijs Douze. Deep clustering for unsupervised learning of visual features. In *Proceedings of the European conference on computer vision (ECCV)*, pages 132–149, 2018. 3
- [6] Mathilde Caron, Ishan Misra, Julien Mairal, Priya Goyal, Piotr Bojanowski, and Armand Joulin. Unsupervised learning of visual features by contrasting cluster assignments. *Advances in neural information processing systems*, 33:9912–9924, 2020. 3
- [7] Guikun Chen, Xia Li, Yi Yang, and Wenguan Wang. Neural clustering based visual representation learning. In *Proceedings of the IEEE/CVF Conference on Computer Vision and Pattern Recognition*, pages 5714–5725, 2024. 3
- [8] Ting Chen, Simon Kornblith, Mohammad Norouzi, and Geoffrey Hinton. A simple framework for contrastive learning of visual representations. In *International conference on machine learning*, pages 1597–1607. PmLR, 2020. 5
- [9] Xin Chen, Biao Jiang, Wen Liu, Zilong Huang, Bin Fu, Tao Chen, and Gang Yu. Executing your commands via motion diffusion in latent space. In *Proceedings of the IEEE/CVF conference on computer vision and pattern recognition*, pages 18000–18010, 2023. 1, 2, 4
- [10] Marco Cuturi. Sinkhorn distances: Lightspeed computation of optimal transport. *Advances in neural information processing systems*, 26, 2013. 4
- [11] Rishabh Dabral, Muhammad Hamza Mughal, Vladislav Golyanik, and Christian Theobalt. Mofusion: A framework for denoising-diffusion-based motion synthesis. In *Proceedings of the IEEE/CVF conference on computer vision and pattern recognition*, pages 9760–9770, 2023. 2
- [12] Chuanghao Ding, Jianrong Zhang, Henghui Ding, Hongwei Zhao, Zhihui Wang, Tengfei Xing, and Runbo Hu. Decoupling with entropy-based equalization for semi-supervised semantic segmentation. In *International Joint Conference on Artificial Intelligence (IJCAI)*, 2023. 3
- [13] Yuhang Ding, Liulei Li, Wenguan Wang, and Yi Yang. Clustering propagation for universal medical image segmentation. In *Proceedings of the IEEE/CVF conference on computer vision and pattern recognition*, pages 3357–3369, 2024. 3
- [14] Tuo Feng, Wenguan Wang, Xiaohan Wang, Yi Yang, and Qinghua Zheng. Clustering based point cloud representation learning for 3d analysis. In *Proceedings of the IEEE/CVF International Conference on Computer Vision*, pages 8283–8294, 2023. 3
- [15] Tuo Feng, Ruijie Quan, Xiaohan Wang, Wenguan Wang, and Yi Yang. Interpretable3d: An ad-hoc interpretable classifier for 3d point clouds. In *Proceedings of the AAAI Conference on Artificial Intelligence*, pages 1761–1769, 2024. 3
- [16] Hichem Frigui and Raghu Krishnapuram. A robust competitive clustering algorithm with applications in computer vision. *Ieee transactions on pattern analysis and machine intelligence*, 21(5):450–465, 2002. 3
- [17] Xuehao Gao, Yang Yang, Zhenyu Xie, Shaoyi Du, Zhongqian Sun, and Yang Wu. Guess: Gradually enriching synthesis for text-driven human motion generation. *IEEE Transactions on Visualization and Computer Graphics*, 30(12):7518–7530, 2024. 2
- [18] Leon A Gatys, Alexander S Ecker, and Matthias Bethge. Image style transfer using convolutional neural networks. In *Proceedings of the IEEE conference on computer vision and pattern recognition*, pages 2414–2423, 2016. 1
- [19] Anindita Ghosh, Noshaba Cheema, Cennet Oguz, Christian Theobalt, and Philipp Slusallek. Synthesis of compositional animations from textual descriptions. In *Proceedings of the IEEE/CVF international conference on computer vision*, pages 1396–1406, 2021. 2
- [20] Purvi Goel, Kuan-Chieh Wang, C Karen Liu, and Kayvon Fatahalian. Iterative motion editing with natural language. In *ACM SIGGRAPH 2024 Conference Papers*, pages 1–9, 2024. 2
- [21] Chuan Guo, Shihao Zou, Xinxin Zuo, Sen Wang, Wei Ji, Xingyu Li, and Li Cheng. Generating diverse and natural 3d human motions from text. In *Proceedings of the IEEE/CVF conference on computer vision and pattern recognition*, pages 5152–5161, 2022. 2, 4, 6, 15
- [22] Chuan Guo, Xinxin Zuo, Sen Wang, and Li Cheng. Tm2t: Stochastic and tokenized modeling for the reciprocal generation of 3d human motions and texts. In *ECCV*, 2022. 2
- [23] Chuan Guo, Yuxuan Mu, Muhammad Gohar Javed, Sen Wang, and Li Cheng. Momask: Generative masked modeling of 3d human motions. In *Proceedings of the IEEE/CVF Conference on Computer Vision and Pattern Recognition*, pages 1900–1910, 2024. 2
- [24] Chuan Guo, Yuxuan Mu, Xinxin Zuo, Peng Dai, Youliang Yan, Juwei Lu, and Li Cheng. Generative human motion stylization in latent space. *arXiv preprint arXiv:2401.13505*, 2024. 2

- [25] Ziyu Guo, Young Yoon Lee, Joseph Liu, Yizhak Ben-Shabat, Victor Zordan, and Mubbasir Kapadia. Stylemotif: Multi-modal motion stylization using style-content cross fusion. *arXiv preprint arXiv:2503.21775*, 2025. 1, 3, 4, 6, 7, 15
- [26] Bo Han, Hao Peng, Minjing Dong, Yi Ren, Yixuan Shen, and Chang Xu. Amd: Autoregressive motion diffusion. In *Proceedings of the AAAI Conference on Artificial Intelligence*, pages 2022–2030, 2024. 2
- [27] Lei Hu, Zihao Zhang, Yongjing Ye, Yiwen Xu, and Shihong Xia. Diffusion-based human motion style transfer with semantic guidance. In *Computer Graphics Forum*, page e15169. Wiley Online Library, 2024. 1, 2, 3
- [28] Xun Huang and Serge Belongie. Arbitrary style transfer in real-time with adaptive instance normalization. In *Proceedings of the IEEE international conference on computer vision*, pages 1501–1510, 2017. 2
- [29] Deok-Kyeong Jang, Soomin Park, and Sung-Hee Lee. Motion puzzle: Arbitrary motion style transfer by body part. *ACM Transactions on Graphics (TOG)*, 41(3):1–16, 2022. 2, 6, 7
- [30] Biao Jiang, Xin Chen, Wen Liu, Jingyi Yu, Gang Yu, and Tao Chen. Motiongpt: Human motion as a foreign language. *Advances in Neural Information Processing Systems*, 36:20067–20079, 2023. 15
- [31] Peng Jin, Yang Wu, Yanbo Fan, Zhongqian Sun, Wei Yang, and Li Yuan. Act as you wish: Fine-grained control of motion diffusion model with hierarchical semantic graphs. *Advances in Neural Information Processing Systems*, 36:15497–15518, 2023. 2
- [32] Jean-Michel Jolion, Peter Meer, and Samira Bataouche. Robust clustering with applications in computer vision. *IEEE transactions on pattern analysis and machine intelligence*, 13(8):791–802, 1991. 3
- [33] Korrawe Karunratanakul, Konpat Preechakul, Supasorn Suwajanakorn, and Siyu Tang. Guided motion diffusion for controllable human motion synthesis. In *Proceedings of the IEEE/CVF International Conference on Computer Vision*, pages 2151–2162, 2023. 2
- [34] Boeun Kim, Jungho Kim, Hyung Jin Chang, and Jin Young Choi. Most: Motion style transformer between diverse action contents. In *Proceedings of the IEEE/CVF Conference on Computer Vision and Pattern Recognition*, pages 1705–1714, 2024. 2
- [35] Boeun Kim, Hea In Jeong, JungHoon Sung, Yihua Cheng, Jeongmin Lee, Ju Yong Chang, Sang-Il Choi, Younggeun Choi, Saim Shin, Jungho Kim, et al. Personabooth: Personalized text-to-motion generation. In *Proceedings of the Computer Vision and Pattern Recognition Conference*, pages 22756–22765, 2025. 2
- [36] Zhe Li, Yisheng He, Lei Zhong, Weichao Shen, Qi Zuo, Lingteng Qiu, Zilong Dong, Laurence Tianruo Yang, and Weihao Yuan. Mulsmo: Multimodal stylized motion generation by bidirectional control flow. *arXiv preprint arXiv:2412.09901*, 2024. 1, 2, 3, 4, 6, 7, 15
- [37] James Liang, Yiming Cui, Qifan Wang, Tong Geng, Wenguan Wang, and Dongfang Liu. Clusterfomer: clustering as a universal visual learner. *Advances in neural information processing systems*, 36:64029–64042, 2023. 3
- [38] James Liang, Tianfei Zhou, Dongfang Liu, and Wenguan Wang. Clustseg: Clustering for universal segmentation. *arXiv preprint arXiv:2305.02187*, 2023. 2, 3
- [39] Xiu Liu, Xinxin Han, Huan Xia, Kang Li, Haochen Zhao, Jia Jia, Gang Zhen, Linzhi Su, Fengjun Zhao, and Xin Cao. Pointcluster: Deep clustering of 3-d point clouds with semantic pseudo-labeling. *IEEE Transactions on Geoscience and Remote Sensing*, 62:1–14, 2024. 3
- [40] Yahui Liu, Bin Tian, Yisheng Lv, Lingxi Li, and Fei-Yue Wang. Point cloud classification using content-based transformer via clustering in feature space. *IEEE/CAA Journal of Automatica Sinica*, 11(1):231–239, 2023. 3
- [41] Yu Lu, Ruijie Quan, Linchao Zhu, and Yi Yang. Zero-shot video grounding with pseudo query lookup and verification. *IEEE Transactions on Image Processing*, 33:1643–1654, 2024. 3
- [42] Ian Mason, Sebastian Starke, and Taku Komura. Real-time style modelling of human locomotion via feature-wise transformations and local motion phases. *Proceedings of the ACM on Computer Graphics and Interactive Techniques*, 5(1):1–18, 2022. 1, 2
- [43] Chenlin Meng, Yutong He, Yang Song, Jiaming Song, Jiajun Wu, Jun-Yan Zhu, and Stefano Ermon. Sedit: Guided image synthesis and editing with stochastic differential equations. *arXiv preprint arXiv:2108.01073*, 2021. 7, 14
- [44] Chuang Niu, Hongming Shan, and Ge Wang. Spice: Semantic pseudo-labeling for image clustering. *IEEE Transactions on Image Processing*, 31:7264–7278, 2022. 3
- [45] Soomin Park, Deok-Kyeong Jang, and Sung-Hee Lee. Diverse motion stylization for multiple style domains via spatial-temporal graph-based generative model. *Proceedings of the ACM on Computer Graphics and Interactive Techniques*, 4(3):1–17, 2021. 2
- [46] Mathis Petrovich, Michael J. Black, and Gül Varol. Action-conditioned 3D human motion synthesis with transformer VAE. In *International Conference on Computer Vision (ICCV)*, 2021. 2
- [47] Mathis Petrovich, Michael J Black, and Gül Varol. Temos: Generating diverse human motions from textual descriptions. In *European Conference on Computer Vision*, pages 480–497. Springer, 2022.
- [48] Mathis Petrovich, Michael J. Black, and Gül Varol. TMR: Text-to-motion retrieval using contrastive 3D human motion synthesis. In *International Conference on Computer Vision (ICCV)*, 2023. 2
- [49] Ekkasit Pinyoanuntapong, Muhammad Usama Saleem, Pu Wang, Minwoo Lee, Srijan Das, and Chen Chen. Bamm: Bidirectional autoregressive motion model. In *Computer Vision – ECCV 2024*, 2024. 2
- [50] Ekkasit Pinyoanuntapong, Pu Wang, Minwoo Lee, and Chen Chen. Mmm: Generative masked motion model. In *Proceedings of the IEEE/CVF Conference on Computer Vision and Pattern Recognition (CVPR)*, 2024. 2
- [51] Ziyun Qian, Dingkan Yang, Mingcheng Li, Dongliang Kou, and Lihua Zhang. Mafd: Fine-grained motion style transfer with adaptive signal fusion. In *ICASSP 2025-2025 IEEE International Conference on Acoustics, Speech and Signal Processing (ICASSP)*, pages 1–5. IEEE, 2025. 1, 2

- [52] Hongyu Qu, Jianan Wei, Xiangbo Shu, and Wenguan Wang. Learning clustering-based prototypes for compositional zero-shot learning. *arXiv preprint arXiv:2502.06501*, 2025. 3
- [53] Sigal Raab, Inbar Gat, Nathan Sala, Guy Tevet, Rotem Shalev-Arkushin, Ohad Fried, Amit Haim Bermano, and Daniel Cohen-Or. Monkey see, monkey do: Harnessing self-attention in motion diffusion for zero-shot motion transfer. In *SIGGRAPH Asia 2024 Conference Papers*, pages 1–13, 2024. 1, 2, 3
- [54] Alec Radford, Jong Wook Kim, Chris Hallacy, Aditya Ramesh, Gabriel Goh, Sandhini Agarwal, Girish Sastry, Amanda Askell, Pamela Mishkin, Jack Clark, et al. Learning transferable visual models from natural language supervision. In *International conference on machine learning*, pages 8748–8763. PmLR, 2021. 3
- [55] Douglas Reynolds. Gaussian mixture models. In *Encyclopedia of biometrics*, pages 827–832. Springer, 2015. 3
- [56] Haim Sawdayee, Chuan Guo, Guy Tevet, Bing Zhou, Jian Wang, and Amit H Bermano. Dance like a chicken: Low-rank stylization for human motion diffusion. *arXiv preprint arXiv:2503.19557*, 2025. 1, 2
- [57] Wenfeng Song, Xingliang Jin, Shuai Li, Chenglizhao Chen, Aimin Hao, Xia Hou, Ning Li, and Hong Qin. Arbitrary motion style transfer with multi-condition motion latent diffusion model. In *Proceedings of the IEEE/CVF Conference on Computer Vision and Pattern Recognition*, pages 821–830, 2024. 1, 2
- [58] Xiangjun Tang, Linjun Wu, He Wang, Bo Hu, Xu Gong, Yuchen Liao, Songnan Li, Qilong Kou, and Xiaogang Jin. Rsmt: Real-time stylized motion transition for characters. In *ACM SIGGRAPH 2023 Conference Proceedings*, pages 1–10, 2023. 1, 2
- [59] Tianxin Tao, Xiaohang Zhan, Zhongquan Chen, and Michiel van de Panne. Style-erd: Responsive and coherent online motion style transfer. In *Proceedings of the IEEE/CVF Conference on Computer Vision and Pattern Recognition*, pages 6593–6603, 2022. 1, 2
- [60] Guy Tevet, Brian Gordon, Amir Hertz, Amit H Bermano, and Daniel Cohen-Or. Motionclip: Exposing human motion generation to clip space. In *European Conference on Computer Vision*, pages 358–374. Springer, 2022. 2
- [61] Guy Tevet, Sigal Raab, Brian Gordon, Yoni Shafir, Daniel Cohen-or, and Amit Haim Bermano. Human motion diffusion model. In *The Eleventh International Conference on Learning Representations*, 2023. 2
- [62] Weilin Wan, Zhiyang Dou, Taku Komura, Wenping Wang, Dinesh Jayaraman, and Lingjie Liu. Tlcontrol: Trajectory and language control for human motion synthesis. In *European Conference on Computer Vision*, pages 37–54. Springer, 2024. 2
- [63] Wenguan Wang, Cheng Han, Tianfei Zhou, and Dongfang Liu. Visual recognition with deep nearest centroids. *arXiv preprint arXiv:2209.07383*, 2022. 3
- [64] Yin Wang, Zhiying Leng, Frederick WB Li, Shun-Cheng Wu, and Xiaohui Liang. Fg-t2m: Fine-grained text-driven human motion generation via diffusion model. In *Proceedings of the IEEE/CVF international conference on computer vision*, pages 22035–22044, 2023. 2
- [65] Mingjie Wei, Xuemei Xie, and Guangming Shi. Acmo: Attribute controllable motion generation. *arXiv preprint arXiv:2503.11038*, 2025. 2
- [66] Yu-Hui Wen, Zhipeng Yang, Hongbo Fu, Lin Gao, Yanan Sun, and Yong-Jin Liu. Autoregressive stylized motion synthesis with generative flow. In *Proceedings of the IEEE/CVF Conference on Computer Vision and Pattern Recognition*, pages 13612–13621, 2021. 2
- [67] Yiming Xie, Varun Jampani, Lei Zhong, Deqing Sun, and Huaizu Jiang. Omnicontrol: Control any joint at any time for human motion generation. *arXiv preprint arXiv:2310.08580*, 2023. 2
- [68] Zhenyu Xie, Yang Wu, Xuehao Gao, Zhongqian Sun, Wei Yang, and Xiaodan Liang. Towards detailed text-to-motion synthesis via basic-to-advanced hierarchical diffusion model. In *Proceedings of the AAAI Conference on Artificial Intelligence*, pages 6252–6260, 2024. 2
- [69] Jingwei Xu, Huazhe Xu, Bingbing Ni, Xiaokang Yang, Xiaolong Wang, and Trevor Darrell. Hierarchical style-based networks for motion synthesis. In *Computer Vision–ECCV 2020: 16th European Conference, Glasgow, UK, August 23–28, 2020, Proceedings, Part XI 16*, pages 178–194. Springer, 2020. 2
- [70] Xueting Yan, Ishan Misra, Abhinav Gupta, Deepti Ghadiyaram, and Dhruv Mahajan. Clusterfit: Improving generalization of visual representations. In *Proceedings of the IEEE/CVF Conference on Computer Vision and Pattern Recognition*, pages 6509–6518, 2020. 3
- [71] Hu Ye, Jun Zhang, Sibio Liu, Xiao Han, and Wei Yang. Ip-adapt: Text compatible image prompt adapter for text-to-image diffusion models. *arXiv preprint arXiv:2308.06721*, 2023. 1
- [72] Ye Yuan, Jiaming Song, Umar Iqbal, Arash Vahdat, and Jan Kautz. Physdiff: Physics-guided human motion diffusion model. In *Proceedings of the IEEE/CVF international conference on computer vision*, pages 16010–16021, 2023. 2
- [73] Jianrong Zhang, Tianyi Wu, Chuanghao Ding, Hongwei Zhao, and Guodong Guo. Region-level contrastive and consistency learning for semi-supervised semantic segmentation. In *International Joint Conference on Artificial Intelligence (IJCAI)*, 2022. 3
- [74] Jianrong Zhang, Yangsong Zhang, Xiaodong Cun, Yong Zhang, Hongwei Zhao, Hongtao Lu, Xi Shen, and Ying Shan. Generating human motion from textual descriptions with discrete representations. In *Proceedings of the IEEE/CVF conference on computer vision and pattern recognition*, pages 14730–14740, 2023. 2
- [75] Jianrong Zhang, Hehe Fan, and Yi Yang. Energymogen: Compositional human motion generation with energy-based diffusion model in latent space. In *Proceedings of the Computer Vision and Pattern Recognition Conference*, pages 17592–17602, 2025. 2, 4, 6
- [76] Lvmin Zhang, Anyi Rao, and Maneesh Agrawala. Adding conditional control to text-to-image diffusion models. In *Proceedings of the IEEE/CVF international conference on computer vision*, pages 3836–3847, 2023. 4

- [77] Mingyuan Zhang, Xinying Guo, Liang Pan, Zhongang Cai, Fangzhou Hong, Huirong Li, Lei Yang, and Ziwei Liu. Remodiffuse: Retrieval-augmented motion diffusion model. In *Proceedings of the IEEE/CVF International Conference on Computer Vision*, pages 364–373, 2023. [2](#)
- [78] Mingyuan Zhang, Zhongang Cai, Liang Pan, Fangzhou Hong, Xinying Guo, Lei Yang, and Ziwei Liu. Motiondiffuse: Text-driven human motion generation with diffusion model. *IEEE transactions on pattern analysis and machine intelligence*, 46(6):4115–4128, 2024. [2](#)
- [79] Zeyu Zhang, Akide Liu, Ian Reid, Richard Hartley, Bohan Zhuang, and Hao Tang. Motion mamba: Efficient and long sequence motion generation. In *European Conference on Computer Vision*, pages 265–282. Springer, 2024. [2](#)
- [80] Chongyang Zhong, Lei Hu, Zihao Zhang, and Shihong Xia. Att2m: Text-driven human motion generation with multi-perspective attention mechanism. In *Proceedings of the IEEE/CVF International Conference on Computer Vision (ICCV)*, pages 509–519, 2023. [2](#)
- [81] Lei Zhong, Yiming Xie, Varun Jampani, Deqing Sun, and Huaizu Jiang. Smoodi: Stylized motion diffusion model. In *European Conference on Computer Vision*, pages 405–421. Springer, 2024. [1](#), [2](#), [3](#), [4](#), [6](#), [7](#), [13](#), [15](#)
- [82] Lei Zhong, Yi Yang, and Changjian Li. Smoogpt: Stylized motion generation using large language models. *arXiv preprint arXiv:2509.04058*, 2025. [1](#)
- [83] Tianfei Zhou, Wenguan Wang, Ender Konukoglu, and Luc Van Gool. Rethinking semantic segmentation: A prototype view. In *Proceedings of the IEEE/CVF conference on computer vision and pattern recognition*, pages 2582–2593, 2022. [2](#), [3](#)
- [84] Zixiang Zhou and Baoyuan Wang. Ude: A unified driving engine for human motion generation. In *Proceedings of the IEEE/CVF conference on computer vision and pattern recognition*, pages 5632–5641, 2023. [2](#)



## Appendix

In this Appendix, we present the following:

- Section A: More Details on Inference.
- Section B: Prototype-based Guidance.
- Section C: Motion Style Transfer.
- Section D: Study of the Loss Function.
- Section E: Impact of Different Similarity Metrics.
- Section F: Study of Hyper-parameters in SMA.
- Section G: Study of Hyper-parameters in Classifier-based Guidance.
- Section H: More Details of Datasets.

### A. More Details on Inference

We adopt the DDIM sampling strategy for the denoising process, with a total of 1000 diffusion steps and a sampling interval of 20. Following SMooDi [81], we employ both classifier-free and classifier-based guidance to improve the quality of stylized motion generation.

#### A.1. Classifier-free Guidance

Classifier-free guidance is a widely used technique in conditional generative models, enabling the model to learn both conditional and unconditional generation behaviors within a single network. During training, conditioning signals (text and style features) are randomly dropped with a certain probability (10%), allowing the model to learn how to interpolate between conditional and unconditional outputs implicitly. During inference, we extend classifier-free guidance to a dual-conditioning setup, where generation is influenced by both content ( $c$ ) and style ( $s$ ). The denoising function is modified to combine unconditional, text-conditioned, and style-conditioned predictions, allowing controllable generation by adjusting the influence of each condition. The denoising function is as follows:

$$\begin{aligned} \epsilon_\theta(z^t, t, c, s) = & \epsilon_\theta(z^t, t, \emptyset, \emptyset) + \\ & w_c(\epsilon_\theta(z^t, t, c, \emptyset) - \epsilon_\theta(z^t, t, \emptyset, \emptyset)) + \\ & w_s(\epsilon_\theta(z^t, t, c, s) - \epsilon_\theta(z^t, t, c, \emptyset)), \end{aligned} \quad (12)$$

where  $w_c$  and  $w_s$  represent the strengths of the classifier-free guidance for the text condition  $c$  and style condition

$s$ , respectively. In our experiments, we set the  $w_c = 7.5$ ,  $w_s = 1$  to balance fidelity and style rendering.

#### A.2. Classifier-based Guidance

To further improve the stylization quality of our Cluster-Style model, we adopt classifier-based guidance following the approach of SMooDi. We train a style feature extractor  $f$  to compute the style representation of both the current denoised motion sample  $x^0$  and the target style reference  $X_s$ . We then compute the  $L_1$  distance between their feature representations and use this signal as a pseudo-loss to optimize the predicted noise. Specifically, at the timestep  $t$  of the diffusion process, we first obtain the current clean latent feature  $z^0$  using DDIM:

$$z^0 = \frac{z^t - \sqrt{1 - \alpha^t} \epsilon_\theta(z^t, t, c, s)}{\sqrt{\alpha^t}} \quad (13)$$

where  $z^t$  is the noisy latent feature at timestep  $t$ ,  $\alpha_t$  is the noise schedule coefficient, and  $c$  and  $s$  denote content feature and style feature respectively. We then define the style guidance term as:

$$G(z^t, t, X_s) = |f(\mathcal{D}(z^0)) - f(X_s)|, \quad (14)$$

which measures the discrepancy between the style of the current sample and the target style. To inject this guidance, we update the predicted noise using the gradient of the guidance term with respect to the latent  $z^t$ :

$$\epsilon_\theta(z^t, t, c, s) = \epsilon_\theta(z^t, t, c, s) + \gamma \nabla_{z^t} G(z^t, t, X_s), \quad (15)$$

where  $\gamma$  is a hyperparameter controlling the strength of the style guidance. In our experiments, we set  $\gamma = 3.0$  and apply it only when the denoising step  $t$  is less than 300.

### B. Prototype-based Guidance

As shown in the visual results of the main paper (Figure 5), our framework is able to generate diverse stylized motion by combining extracted features with different prototypes. Our prototype-based guidance can be categorized into two types: global guidance and local guidance. Specifically, at diffusion timestep  $t$ , we can estimate the current clean sample  $z^0$  from noisy latent  $z^t$  and  $t$  using Eq 13, and use the VAE decoder  $\mathcal{D}$  to obtain the motion  $x^0 = \mathcal{D}(z^0)$ . We then compute the style feature  $f_s^0 = [f_g^0, f_{l,1}^0, f_{l,2}^0 \dots f_{l,L_w}^0]$  of  $x_0$  and rewrite the original formulation  $G(z^t, t, X_s)$  in Eq. 14. For global prototype-based guidance, the guidance formulation (Eq. 14) is updated as:

$$G_p(z^t, t, p_s^k) = 1 - \cos(f_g^0, p_s^k), \quad (16)$$

where  $p_s^k$  is the  $k$ -th global prototype feature of style category  $s$ ,  $f_g^0$  is the global feature of  $x_0$ , and  $\cos(\cdot)$  denotes

$\lambda_{\text{style}}$	FID ↓	FSR ↓	MM Dist ↓	R-Precision (Top-3) ↑	Diversity →	SRA ↑
0.5	1.093	0.110	3.597	0.711	8.613	75.046
1	1.137	0.113	3.619	0.708	8.719	78.101
2	1.546	0.139	4.012	0.631	8.695	83.247

Table 5. Ablation study on the impact of  $\lambda_{\text{style}}$  in stylized motion generation.

the cosine similarity. For local prototype-based guidance, we can use different  $k_i$ -th local prototype  $p_{s,l}^{k_i,i}$  for each temporal segment  $i$  and the formulation is updated as:

$$G_l(z^t, t, [p_{s,l}^{k_1,1}, p_{s,l}^{k_2,2}, \dots, p_{s,l}^{k_{L_w}, L_w}]) = \sum_{i=1}^{L_w} (1 - \cos(f_{l,i}^{x^0}, p_{s,l}^{k_i,i})), \quad (17)$$

where  $f_{l,i}^{x^0}$  is the local feature of the  $i$ -th segment in  $x^0$ , and  $L_w$  is the number of segments.

We use Eq. 15 to iteratively optimize  $z^t$ . This approach not only enables the generation of diverse results within the same style but also facilitates the understanding of sub-style patterns captured by different prototypes.

### C. Motion Style Transfer

Inspired by SDEdit [43], we perturb a content motion  $X_c \in \mathbb{R}^{L_c \times D}$  by encoding it into a latent feature  $z^0$  via the VAE and adding Gaussian noise over  $T'$  steps using the same noise schedule as in training, obtaining  $z^{T'}$ . We then apply conditional denoising with the pretrained ClusterStyle model, guided by the style feature  $f_s$ , to progressively inject style-specific patterns while maintaining the original motion structure. The refined latent feature  $\hat{z}^0$  is finally decoded by the VAE decoder  $\mathcal{D}$  to produce the transferred motion result  $x_s^0 = \mathcal{D}(\hat{z}^0)$ .

During the denoising stage, we utilize both classifier-free guidance and classifier-based guidance to enhance the performance of the results further. The denoising function is modified as follows:

$$\epsilon_\theta(z^t, t, \emptyset, f_s) = \epsilon_\theta(z^t, t, \emptyset, \emptyset) + w_s(\epsilon_\theta(z^t, t, \emptyset, f_s) - \epsilon_\theta(z^t, t, \emptyset, \emptyset)). \quad (18)$$

For enhanced clarity, Algorithm 1 presents the pseudo code for the motion style transfer component. In the experiment, we set the  $w_s = 2.25$ ,  $T' = 500$ ,  $\gamma = 2.5$ .

### D. Study of the Loss Function

During training, we adopt a composite loss function defined as follows:

$$\mathcal{L}_{\text{total}} = \mathcal{L}_{\text{diff}}^s + \mathcal{L}_{\text{diff}}^c + \lambda_{\text{style}} \mathcal{L}_{\text{style}}. \quad (19)$$

This design aims to preserve the prior knowledge of motion generation learned by the diffusion model from the HumanML3D dataset, while enabling it to additionally learn

#### Algorithm 1 Algorithm of Motion Style Transfer

**Require:** A motion diffusion model  $M$ , a style encoder model  $F$ , a VAE encoder  $\mathcal{E}$  and decoder  $\mathcal{D}$ , a content motion  $X_c$ , a style motion  $X_s$ , a DDIM sampling method  $S$ , noise variance schedule  $\alpha$  and timesteps set  $\mathcal{T}$ , and a style guidance function  $G$ .

```

1:  $z^{\text{start}} = \mathcal{E}(X_c)$ 
2:  $s = F(X_s)$ 
3:  $z \sim \mathcal{N}(0, I)$ 
4:  $z^{T'} = \sqrt{\alpha^{T'}} z^{\text{start}} + \sqrt{1 - \alpha^{T'}} z$ 
5: for each  $t \in \mathcal{T}$  do
6:    $\epsilon_t = (1 - w_s)M(z^t, t, \emptyset, \emptyset) + w_s M(z^t, t, \emptyset, s)$ 
7:    $\epsilon_t = \epsilon_t + \gamma \nabla_{z^t} G(z^t, t, s)$ 
8:    $z^{t-1} \sim S(z^t, \epsilon_t, t)$ 
9: end for
10:  $x^0 = \mathcal{D}(z^0)$ 
11: return  $x^0$ 

```

style-related motion features from the 100STYLE dataset. We investigate the influence of different values of  $\lambda_{\text{style}}$  on the overall performance. As shown in Table 5, when  $\lambda_{\text{style}} = 2$ , the model focuses heavily on optimizing the style-related objective. This trade-off is reflected in the deterioration of metrics such as R-precision, FID, and MM-Distance. On the other hand, when  $\lambda_{\text{style}} = 0.5$ , the model pays insufficient attention to style guidance, resulting in a significant drop in style relevance, as indicated by lower SRA scores. To balance both content fidelity and style consistency, we adopt  $\lambda_{\text{style}} = 1$  in our final experiments, achieving more stable and well-rounded performance across evaluation metrics.

### E. Impact of Different Similarity Metrics

In the main paper, we use the cosine similarity to measure the similarity in the prototype-based contrastive learning loss. However, other similarity metrics can also be applied in this context. In this section, we investigate the impact of using alternative metrics, specifically the  $L_2$  and  $L_1$  distances, and compare their performance with cosine similarity. As shown in Table 7, adopting either  $L_1$  or  $L_2$  similarity metrics leads to a decrease in SRA. In particular, using  $L_1$  distance as the similarity metric further drops in FID and Top-3, indicating a decline in overall motion quality and

$\lambda$	FID ↓	FSR ↓	MM Dist ↓	R-Precision(Top-3) ↑	Diversity →	SRA ↑
0.5	1.175	0.111	3.619	0.701	8.569	77.030
1.0	1.141	0.113	3.612	0.703	8.726	77.213
learnable	1.137	0.113	3.619	0.708	8.719	78.101

Table 6. Ablation study on the impact of  $\lambda$  in stylized motion generation.

sim	FID ↓	FSR ↓	R-Precision ↑ (Top-3)	Diversity →	SRA ↑
$L_2$	1.191	0.114	0.706	8.553	76.483
$L_1$	1.322	0.119	0.689	8.936	76.802
cos	1.137	0.113	0.708	8.719	78.101

Table 7. Ablation study of different similarity metrics.

$\gamma$	FID ↓	MM Dist ↓	R-Precision ↑ (Top-3)	Diversity →	SRA ↑
2	0.695	3.412	0.743	8.727	66.645
2.5	0.858	3.498	0.731	8.549	72.287
3.0	1.137	3.619	0.708	8.719	78.101
3.5	1.243	3.698	0.699	8.622	79.807
4	1.370	3.719	0.695	8.199	81.771

Table 8. Effect of classifier-based guidance strength  $\gamma$ .

content alignment.

## F. Study of Hyper-parameters in SMA

We further explore the role of the balancing coefficient  $\lambda$  in our SMA. Specifically, we compare two strategies for setting  $\lambda$ : (1) using a fixed constant value, and (2) learning  $\lambda$  as a trainable parameter during optimization. Results in Table 6 demonstrate that the trainable variant consistently yields superior overall performance across multiple evaluation metrics. This suggests that adaptively learning  $\lambda$  enables the model to better coordinate between content fidelity and style consistency depending on the data characteristics at each stage of training.

## G. Study of Hyper-parameters in Classifier-based Guidance

We investigate the impact of  $\gamma$ . We try the different values of the parameter  $\gamma$ , as shown in Table 8. We observe that as  $\gamma$  increases, both FID and text-motion alignment metrics (e.g., R-Precision and MM-Dist) tend to degrade, while the Style Relevance Accuracy (SRA) consistently improves. These results indicate that the  $\gamma$  serves as a trade-off coefficient between content alignment and style consistency. In our final experiments, we set  $\gamma = 3$  to strike a balance between these two aspects.

## H. More Details of Datasets

Our experiments are conducted on two datasets: HumanML3D [21] and 100STYLE [81].

**HumanML3D.** HumanML3D is a large-scale, text-to-motion dataset introduced to facilitate research in generating realistic human motions from texts. It contains approximately 14,616 motion clips paired with 44,970 text descriptions, covering a wide range of daily activities such as walking, sitting, jumping, gesturing, and complex sequences like dancing or interacting with objects. Motions are represented in the SMPL format and captured at 20 FPS. The dataset emphasizes semantic alignment between language and motion, making it well-suited for evaluating both diversity and accuracy in language-conditioned motion generation. In our experiments, the pretrained text-to-motion diffusion is trained on HumanML3D. Following prior works [25, 36, 81], we adopt the same test set motions or texts as contents for evaluation.

**100STYLE.** The 100STYLE dataset is the largest motion style dataset to date, containing approximately 1,125 minutes of motion sequences across 100 diverse locomotion styles. To align it with HumanML3D, 100STYLE retargets all motion sequences to the SMPL format and applies the same preprocessing pipeline used for HumanML3D. It also leverages MotionGPT [30] to generate pseudo-text descriptions for each style motion sequence. Following SMooDi [81], we adopt the same training and testing data split by selecting 47 style categories.